



Phytosomal Delivery of Wedelolactone Isolated from Eclipta Extract: Formulation, Characterization, and Anticancer Potential

PRACHI MAHESHWARI^{1*} and VIVEK DANIEL¹

¹Faculty of Pharmacy, Oriental University Indore, M.P. 452001, India

*Corresponding author E-mail: prachipharma86@gmail.com

<http://dx.doi.org/10.13005/ojc/420210>

(Received: August 25, 2025; Accepted: February 05, 2026)

ABSTRACT

The present study was designed to enhance the therapeutic efficacy and bioavailability of wedelolactone isolated from *Eclipta alba* leaf extract through phytosomal encapsulation and to evaluate its anticancer potential against breast cancer. Wedelolactone-loaded phytosomes were prepared using the nanoprecipitation technique and comprehensively characterized by dialysis membrane diffusion studies and dynamic light scattering. Critical physicochemical parameters, including particle size, polydispersity index, zeta potential and drug encapsulation were systematically evaluated. In vitro drug release behavior was investigated, and cytotoxic and antiproliferative activities were assessed using the MTT assay against 4T1 murine breast cancer cells. Acute oral toxicity and anticancer activity was evaluated in Swiss albino mice. The optimized phytosomal formulation exhibited a mean particle size of 584 ± 0.15 nm, a zeta potential of -23.8 ± 1.2 mV, and a PDI of 0.4 ± 0.002 , indicating acceptable stability and size uniformity. Encapsulation efficiency was found to be $89.75 \pm 1.70\%$. In vitro release studies demonstrated an initial burst followed by sustained drug release. The wedelolactone-loaded phytosomes showed significantly enhanced antiproliferative activity against 4T1 cells, with an IC₅₀ value of 67.8 ± 2.4 $\mu\text{g/mL}$ ($p < 0.001$). Acute toxicity studies confirmed the formulation's safety up to a dose of 400 mg/kg. Furthermore, in vivo evaluation revealed a tumor inhibition of 60.9% following treatment with wedelolactone phytosomes. We can conclude that phytosomal encapsulation of isolated wedelolactone markedly improved its anticancer efficacy while maintaining a favorable safety profile, highlighting its promising potential as an advanced nanocarrier-based therapeutic strategy for breast cancer management.

Keywords: Phytosomes, Nanoprecipitation, Cancer, 4T1 cells, MTT assay, Wedelolactone.



INTRODUCTION

Breast cancer remains the leading cause of cancer-related mortality among women worldwide, representing a significant global public health challenge^[1,2]. In 2020, approximately 2.3 million new cases and 685,000 deaths were reported globally, with developing countries bearing a disproportionate share of this burden^[1,2]. Limited access to early diagnosis and advanced treatment modalities in low- and middle-income countries contributes to a higher mortality-to-incidence ratio^[3]. The escalating incidence of breast cancer in these regions has been linked to changing reproductive patterns, lifestyle transitions, and increased life expectancy^[4]. Although conventional adjuvant therapies such as chemotherapy, immunotherapy, and radiotherapy have substantially improved clinical outcomes, their application is frequently limited by severe adverse effects, the emergence of drug resistance, and high treatment costs, particularly in resource-limited settings^[5,6]. These challenges underscore the urgent need for alternative, effective, and economically viable therapeutic strategies.

Natural products derived from medicinal plants have emerged as a valuable source of anticancer agents, often exhibiting multitargeted mechanisms of action with reduced systemic toxicity. The clinical success of plant-derived chemotherapeutic agents, such as docetaxel from *Taxus baccata*, highlights the therapeutic relevance of phytochemicals in cancer management. Among such medicinal plants, *Eclipta alba* (Bhringaraj) has garnered significant attention due to its promising anticancer potential^[7,8]. *Eclipta alba* is rich in bioactive phytoconstituents, including wedelolactone, apigenin, ursolic acid, oleanolic acid, luteolin, and eclalbasaponins, which collectively contribute to its pharmacological profile^[8]. Notably, wedelolactone—a coumestan derivative has been identified as one of the principal bioactive compounds responsible for the plant's anticancer activity.

Preclinical studies have demonstrated that *Eclipta alba* extracts and wedelolactone can inhibit the proliferation of various cancer cell lines, including breast and colon cancer cells^[7,9]. The anticancer mechanisms attributed to wedelolactone include the

induction of apoptosis, suppression of angiogenesis, modulation of inflammatory pathways, and inhibition of key signaling molecules involved in tumor growth and metastasis^[7]. Importantly, alcoholic extracts of *Eclipta alba* have shown potent antioxidant and anticancer activities without inducing significant toxicity, further supporting their therapeutic safety^[9]. Nevertheless, wedelolactone's low bioavailability and restricted water solubility hinder its clinical translation, albeit its encouraging pharmacological profile.

Nanomedicine offers innovative solutions to overcome these limitations by improving the delivery, stability, and therapeutic efficacy of anticancer agents^[10-12]. Nanoparticles, typically ranging from 1 to 100 nm in size, can be engineered to function as efficient drug delivery systems, enhancing tumor targeting while minimizing systemic toxicity^[13,14]. Within this context, phytosomes hybrid nanostructures formed by complexing phytoconstituents with phospholipids—have emerged as a promising nanocarrier system^[15-18]. Phytosomes enhance the lipophilicity of plant-derived compounds, facilitating their passage across lipid-rich biological membranes and thereby improving bioavailability.

In cancer therapy, phytosomal formulations can passively target tumor tissues via the enhanced permeability and retention (EPR) effect, which allows preferential accumulation of nanoparticles in tumor sites due to leaky vasculature^[19]. Moreover, phytosomes offer protection of encapsulated bioactives from enzymatic degradation, sustained drug release, improved therapeutic efficacy, and reduced toxicity^[20,21]. These attributes make phytosomes particularly attractive for the delivery of poorly bioavailable phytochemicals such as wedelolactone.

Collectively, the potent anticancer activity of wedelolactone derived from *Eclipta alba*, combined with the advanced drug delivery capabilities of phytosomal nanocarriers, represents a promising and innovative strategy for the development of effective, safe, and affordable breast cancer therapeutics.

MATERIALS AND METHODS

High-purity dichloromethane, hexane, chloroform and ethanol were procured from SD Fine Chemicals (Indore, India). Soy phosphatidylcholine was obtained from Qualigens Chemicals (India). The MTT reagent and TRIzol® reagent were purchased from Sigma-Aldrich (Mumbai, India). The 4T1 murine mammary carcinoma cell line were procured from the CCMB, Pune, India. Cell culture media and supplements, including Dulbecco's Modified Eagle Medium (DMEM), fetal bovine serum (10%), L-glutamine (1%), and antibiotic solution (1%), were procured from Rankem, India.

Preparation of extract

We obtained the fresh *Eclipta alba* leaves from Shobhasavi Ayurvedics and Agros in Bhopal, India, and the Department of Botany at Shri Krishna University verified their authenticity. The procured leaves were dried in air at room temperature for one week and subsequently pulverized into a coarse powder. Soxhlet extraction was employed to efficiently isolate bioactive constituents from the powdered plant material^[22]. Briefly, 200 g of the powdered leaves were extracted with ethanol in Soxhlet apparatus for 72 hours, maintaining the extraction temperature at 50°C.

Isolation of Wedelolactone

The ethanolic extract of *Eclipta alba* (15 g) was processed using column chromatography to isolate wedelolactone. The crude extract was adsorbed onto silica gel (60-120 mesh) and loaded onto a glass column packed with a silica gel slurry prepared in hexane, followed by sequential elution with solvents of increasing polarity, namely hexane, chloroform, ethyl acetate, and methanol, to achieve polarity-based separation of phytoconstituents. Elution was performed using 100-200 mL of each solvent and fractions of 20 mL were collected and monitored by thin-layer chromatography using chloroform:methanol (9:1, v/v) as the mobile phase. Fractions exhibited a prominent spot with an R_f value of approximately 0.52, were therefore pooled and concentrated. The resulting semi-solid residue was further purified by recrystallization from hot methanol to yield yellow crystalline wedelolactone^[22].

Phytosome Preparation

Wedelolactone-loaded phytosomes were prepared using the thin-layer hydration

technique as previously reported^[23]. Briefly, soy phosphatidylcholine was dissolved in dichloromethane, while wedelolactone was separately dissolved in 90% ethanol in the proportions indicated in Table 1. The two solutions were combined in a RBF and sonicated for 10 min to ensure uniform mixing and promote complex formation.

The resulting mixture was subjected to solvent evaporation using a Büchi Mini Spray Dryer B-290, wherein controlled nitrogen gas flow, inlet and outlet temperatures of 100°C, and appropriate pump and aspirator settings facilitated efficient removal of organic solvents. This process led to the formation of a thin, uniform film of the wedelolactone phytosomal complex. The thin-layer hydration method was selected due to its simplicity, reproducibility, and effectiveness in producing homogeneous and stable phytosome formulations.^[23]

Table 1: Composition of Phytosome Formulation of Isolated wedelolactone

Phytosomes Formulation code	Molar ratio (Egg lecithin: Cholesterol: isolated wedelolactone)	Chloroform (ml)
F1	1:0.5:1	10
F2	2:1:1	10
F3	1:0.5:2	10
F4	2:1:2	10

Characterization of Wedelolactone Phytosomes

Percentage Entrapment Efficiency

The entrapment efficiency (%EE) of wedelolactone within the phytosomal complex was determined by ultracentrifugation as described previously^[24]. The phytosome dispersion was centrifuged at 15,000 rpm for 90 min at 4°C, following which the supernatant containing the unencapsulated drug was carefully collected. The amount of free wedelolactone in the supernatant was quantified by UV-visible spectrophotometry at 351 nm. The measured concentration of untrapped wedelolactone was used to calculate the percentage entrapment efficiency according to standard methods^[25].

Zeta Potential, Polydispersity Index, and Particle

Size Distribution

Dynamic light scattering (DLS) analysis was carried out using a Malvern Zetasizer Nano system to determine the particle size distribution, zeta potential, and polydispersity index (PDI) of the phytosomal complex [26,27]. Measurements were performed under standardized conditions, including a temperature of 25°C, appropriate laser wavelength and scattering angle, and predefined refractive index and viscosity settings of the dispersant, as specified by the instrument software [28].

In Vitro Drug Release of wedelolactone from Prepared Phytosomes

Wedelolactone phytosomes were tested for their in vitro drug release characteristics using a modified dynamic dialysis approach. A pH 7.4 phosphate-buffered saline solution with a molecular weight cutoff of 4000 Da was used as the release medium in the dialysis bag. Ten milligrammes of phytosomes and two millilitres of PBS were combined in the dialysis bag. Afterwards, 100 mL of PBS was added to the bag, and the mixture was swirled at 100 rpm in an Erlenmeyer flask while being held at 37°C. At 0, 8, 12, 24, and 72 hours, fresh PBS was added to replace the whole release medium. This process was prepared. The collected sample underwent filtering using a 0.45 µm Millipore filter. The amount of released wedelolactone in the filtrate was determined by spectrophotometer at 351 nm, with fresh PBS serving as a reference [31].

Cell Viability Test

The MTT assay was used to investigate the cytotoxic activity of wedelolactone phytosomes against the 4T1 murine mammary cancer cell lines [32,33]. In a nutshell, cells that were multiplying exponentially were trypsinized, counted by trypan blue exclusion, and then seeded in 96-well microtiter plates with 100 µL of minimum necessary media and 10% fetal bovine serum at a density of 1×10^5 cells/mL. Cells were treated with wedelolactone phytosomes with increasing concentrations (10–100 µg/mL) after incubating them for 24 hours at 37°C in a humidified environment with 5% CO₂. The wells were supplemented three times with progressively diluted phytosomes, beginning at a concentration of 100 µL. The plates were incubated at 37°C for an

extra 2 hours after being incubated for 72 hours, after which 50 µL of MTT dye was added to every well. To dissolve the formazan crystals produced by live cells, 100 µL of dimethyl sulfoxide was added later. Utilizing a Thermo Fisher Multiskan Go Spectrophotometer, the absorbance was ascertained at 570 nm. As a positive control, doxorubicin was used. The term CC₅₀, which stands for the concentration that causes 50% cell death, was used to express the cytotoxicity compared to the untreated cells (the negative control). The IC₅₀ of wedelolactone phytosomes against 4T1 cells was calculated with the help of GraphPad Prism 6.

In Vivo Acute Toxicity Study

Female Swiss albino mice weighing 18–22 g and kept in a controlled environment with a temperature of 25°C and lighting provided by the PBRI animal house were utilized in this study. The mice were allowed free access to food and drink. Each of the nine groups consisted of six mice per group, who were identified by their unique tail marks. Following OECD recommendations with minor adjustments, the acute toxicity research was carried out [34,35].

The mice were given a single oral dosage of the test drug in PBS at concentrations of 50, 300, or 2000 mg/kg body weight, administered at a volume of 0.2 mL, after a 3-hour fasting period during which they were given water as they needed it. The first five hours of each observation were devoted to tracking general behavior, changes in body weight, and death; subsequent assessments were performed daily for the duration of the study. The following parameters were included in these observations: death rate, symptoms of acute toxicity, behavioral changes (such as aggression, paralysis, vocalization, restlessness, agitation, convulsions, ataxia, diarrhea, piloerection, catatonia, altered locomotion, grooming, fasciculation, sleep patterns, coma, prostration, hypoxia, hyperactivity) [36]. Day 1, 7, and 14 were the days when body weights were recorded. After 14 days of observation, the animals were put to sleep and a necropsy was conducted. We looked for obvious problems in the brain, ovaries, liver, kidneys, spleen, lungs, and intestines [37–38].

Anticancer Potential of Isolated Wedelolactone Phytosomes

To evaluate the in-vivo effectiveness of wedelolactone phytosomes, we have utilised the 4T1 syngenic mouse model, which more closely resembles human breast cancer in an immune-competent state. Mammary cancer of the mice We allowed 4T1 cells to grow into palpable tumours in female Balb/c mice that were 4 to 6 weeks old by injecting them subcutaneously into the mammary fat pad on the right flank. A two-week course of treatment included an intravenous injection once daily. Table 2 shows that the experimental group of mice were intravenously injected with wedelolactone phytosomes suspended in normal saline solution, while the control group of mice were given only normal saline solution. An electronic digital calliper was used to measure the tumour size at regular intervals. Once the study came to a close, the mice were killed [39-40].

Table 2: Treatment protocol for breast cancer induced mice

Groups	Treatment
Group I	Normal control i.e. Normal saline solution
Group II	Standard (Doxorubicin 2mg/kg), iv injection
Group III	Treated with isolated wedelolactone (100 mg/kg)
Group IV	Treated with Wedelolactone Phytosomes (100mg/kg)

RESULTS AND DISCUSSION

The Soxhlet extraction method produced a dark brown extract of *Eclipta alba* with a notable yield of 12.65% w/w. This relatively high extraction efficiency is attributed to the continuous solvent circulation inherent to the Soxhlet system, which ensures sustained contact between the fresh solvent and plant material, thereby facilitating the exhaustive extraction of bioactive phytoconstituents. The percentage yield of wedelolactone from the ethanolic extract of *Eclipta alba* was found to be 67.18%, which is considered significantly high for the isolation of a specific phytoconstituent. This high yield can be attributed to efficient solvent extraction by ethanol. The use of ethanol likely enhanced solubilization and extraction

efficiency of wedelolactone from plant material. The wedelolactone obtained was subsequently utilized for the formulation of phytosomes [41-42].

Percentage Encapsulation Efficiency

Formulation F2 exhibited the highest entrapment efficiency of $89.75 \pm 1.70\%$, indicating an optimal phospholipid-to- isolated wedelolactone ratio that facilitated maximum incorporation of the active phytoconstituents within the lipid bilayer. Other formulations F1, F3 and F4 shown an EE (%) of 82.30 ± 1.52 , 77.43 ± 1.25 and 78.67 ± 1.38 respectively [43-45].

Particle Size, Polydispersity Index and Zeta Potential

Hydrodynamic diameter of phytosomes, obtained from five DLS measurements, ranged from 584.1 nm (Table 3). This size range falls within the microsphere category (< 500 nm). The polydispersity index, ranging from 0.116 ± 0.003 to 0.208 ± 0.015 , indicates a homogeneous particle size distribution, consistent with the criterion for optimal homogeneity (PDI < 0.5) [45].

Table 3: Vesicle Diameter Readings of Isolated Wedelolactone Phytosome Formulations

Formulation Code	Vesicle Diameter Mean \pm SD (nm)
F1	604.0 ± 10.2
F2	584.1 ± 3.6
F3	597.2 ± 6.9
F4	594.2 ± 7.6

The measured zeta potential for F2 was -23.8 mV. Formulation F1, F3 and F4 shown zeta potential -22.2 ± 1.4 , -22.4 ± 1.1 and -23.4 ± 0.6 . Although slightly below the ideal threshold of -30 mV, this negative surface charge still indicates moderate stability and suggests a reasonable degree of electrostatic repulsion preventing immediate aggregation. [46-49].

In Vitro Drug Release Study

Formulation F2 exhibited a sustained and controlled release profile, with approximately $82.6 \pm 1.3\%$ of the drug released over 12 hours,

compared to a more rapid release observed in other formulations (Figure 1). This indicates the efficient encapsulation and gradual release behavior of the phytoconstituents from the phytosomal matrix. The sustained release effect observed in F2 makes it a promising candidate for prolonged therapeutic action. Formulation F2 demonstrated the most sustained drug release profile, suggesting its potential for long-acting therapeutic applications. [50-52]. The release data was most closely matched by the Korsmeyer-Peppas model ($R^2 = 0.9306$) among the kinetic models that were tested. Consistent with previous findings and typical of controlled-release systems, this points to the presence of erosion and diffusion as governing processes for drug release [53].

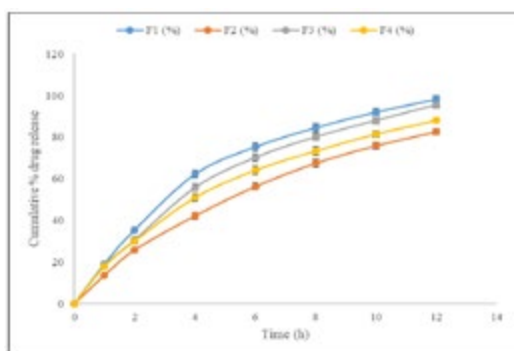


Figure 1. Comparison of In vitro Drug Release (%) of Isolated Wedelolactone Phytosomal Formulations (F1-F4)

Cytotoxicity Studies

The phytosomal formulation exhibited significantly lower IC values across the cell lines compared to the crude isolated wedelolactone, indicating enhanced cytotoxic activity.

Table 4: In vitro Cytotoxicity (MTT Assay) of Isolated Wedelolactone Phytosomal Formulation and Isolated Wedelolactone against Breast Cancer Cell Lines

Conc. (µg/mL)	4T1
10	91.4 ± 2.1
25	79.1 ± 2.0
50	63.8 ± 2.5
75	47.2 ± 2.3
100	34.9 ± 1.8
IC (µg/mL)	67.8 ± 2.4

In Vivo Toxicity Studies

At lower doses (50 and 100 mg/kg), no signs of toxicity or behavioral abnormalities were observed. At 200 mg/kg, mild signs such as temporary lethargy and reduced locomotor activity were noted within the first 24 hours, which resolved spontaneously. However, at 400 mg/kg, moderate toxicity signs (e.g., piloerection, labored breathing, and transient convulsions) were observed, and 1 out of 6 animals died, suggesting a dose-dependent response.

In vivo Anticancer Potential of Wedelolactone Phytosomal Formulation

Animals treated with the wedelolactone phytosome formulation exhibited a marked and statistically significant reduction in tumor progression when compared with both the untreated control group and the group receiving crude isolated wedelolactone ($p < 0.01$). By day 21, the mean tumor volume in the phytosome-treated group was limited to $410.3 \pm 28.4 \text{ mm}^3$, indicating substantial inhibition of tumor growth. In contrast, animals treated with crude isolated wedelolactone showed a considerably higher mean tumor volume of $756.5 \pm 34.2 \text{ mm}^3$, while the control group demonstrated rapid and uncontrolled tumor growth, reaching $1050.2 \pm 41.7 \text{ mm}^3$ (Table 5).

Table 5: In vivo Anticancer Activity of Isolated Wedelolactone Phytosomes in 4T1 Tumor-Bearing Mice

Group	Tumor Volume (mm³) (Day 21)	Body Weight (g) (Day 21)	% In-hibition	Survival Rate (%)
Control (Saline)	1056.2 ± 41.7	23.4 ± 1.2	—	66.7
Doxorubicin (2 mg/kg)	395.7 ± 25.1	21.5 ± 1.5	62.5%	100.0
Crude isolated wedelolactone (100 mg/kg)	769.5 ± 34.2	24.6 ± 1.0	27.1%	83.3
Phytosome (100 mg/kg)	412.3 ± 28.4	25.8 ± 1.3	60.9%	100.0

($p < 0.01$, ± SD; n = 6)

CONCLUSIONS

The development of wedelolactone phytosomes addresses the limitations of conventional herbal extracts by enhancing solubility, bioavailability, and stability, thereby improving therapeutic efficacy. Comprehensive in vitro and in vivo studies have confirmed the safety and efficacy of wedelolactone phytosomes, demonstrating their potential as a promising therapeutic agent.

The absence of acute toxicity and adverse effects at high doses further strengthens their potential for clinical translation. Future research should focus on long-term toxicity studies, detailed mechanistic investigations, and clinical trials to fully realize the therapeutic benefits of wedelolactone phytosomes.

Funding

There was no outside support for this study.

Data Availability Statement

Data generated is included in manuscript.

Conflicts of Interest

There is no conflict of interest.

Acknowledgements

The authors wish to express their gratitude to the Faculty of Pharmacy at Oriental University Indore, who provided invaluable support and the necessary resources to conduct the research.

Author Contributions

Conceptualization and project execution: Vivek Daniel; Initial draft preparation, review, and editing: Prachi Maheshwari.

REFERENCES

- Lancet, N. *Lancet*, **2009**; 374(9701): 1567. [https://doi.org/10.1016/s0140-6736\(09\)61930-9](https://doi.org/10.1016/s0140-6736(09)61930-9)
- Ghoncheh, M.; Momenimovahed, Z.; Salehiniya, H. *Asian Pac. J. Cancer Prev.*, **2016**; 17(S3): 47–52. <https://doi.org/10.7314/apjcp.2016.17.s3.47>
- Vieira, R.A.C.; Biller, G.; Uemura, G.; Ruiz, C.A.; Curado, M.P. *Clinics*, **2017**; 72(4): 244–253. [https://doi.org/10.6061/clinics/2017\(04\)09](https://doi.org/10.6061/clinics/2017(04)09)
- Al-Asadi, J.N.; Al-Mayah, S.M. *Oman Med. J.*, **2020**; 35(4): e147. <https://doi.org/10.5001/omj.2020.66>
- Tfayli, A.; Temraz, S.; Mrad, R.A.; Shamseddine, A. *J. Oncol.*, **2010**; 490631. <https://doi.org/10.1155/2010/490631>
- Unger-Saldaña, K. *World J. Clin. Oncol.*, **2014**; 5(3): 465. <https://doi.org/10.5306/wjco.v5.i3.465>
- Yadav, N.K.; Arya, R.K.; Dev, K.; Sharma, C.; Hossain, Z.; Meena, S.; et al. *Oxid. Med. Cell. Longev.*, **2017**; 9094641. <https://doi.org/10.1155/2017/9094641>
- Jahan, R.; Al-Nahain, A.; Majumder, S.; Rahmatullah, M. *ISRN Pharmacol.*, **2014**; 385969. <https://doi.org/10.1155/2014/385969>
- Nelson, V.K.; Sahoo, N.K.; Sahu, M.; Sudhan, H.H.; Pullaiah, C.P.; Muralikrishna, K.S. *BMC Complement. Med. Ther.*, **2020**; 20(1): 1–10. <https://doi.org/10.1186/s12906-020-03118-9>
- Fan, D.; Cao, Y.; Cao, M.; Wang, Y.; Cao, Y.; Gong, T. *Signal Transduct. Target. Ther.*, **2023**; 8(1). <https://doi.org/10.1038/s41392-023-01536-y>
- Vinogradov, S.; Wei, X. *Nanomedicine*, **2012**; 7(4): 597–615. <https://doi.org/10.2217/nnm.12.22>
- Ferrari, M. *Nat. Rev. Cancer*, **2005**; 5(3): 161–171. <https://doi.org/10.1038/nrc1566>
- Vlamidis, Y.; Voliani, V. *Front. Bioeng. Biotechnol.*, **2018**; 6: 143. <https://doi.org/10.3389/fbioe.2018.00143>
- Shi, J.; Kantoff, P.W.; Wooster, R.; Farokhzad, O.C. *Nat. Rev. Cancer*, **2017**; 17(1): 20–37. <https://doi.org/10.1038/nrc.2016.108>
- Manandhar, S.; Sjöholm, E.; Bobacka, J.; Rosenholm, J.M.; Bansal, K.K. *J. Nanotheranostics*, **2021**; 2(1): 63–81. <https://doi.org/10.3390/jnt2010005>
- Xie, J.; Yang, Z.; Zhou, C.; Zhu, J.; Lee, R.J.; Teng, L. *Biotechnol. Adv.*, **2016**; 34(4): 343–353. <https://doi.org/10.1016/j.biotechadv.2016.04.002>
- Bai, Y.Y.; Zheng, S.; Zhang, L.; Xia, K.; Gao, X.; Li, Z.H.; et al. *J. Biomed. Nanotechnol.*, **2014**; 10(11): 3351–3360. <https://doi.org/10.1166/jbn.2014.1994>
- El-Sahli, S.; Hua, K.; Sulaiman, A.; Chambers, J.; Li, L.; Farah, E.; et al. *Cell Death Dis.*, **2021**;

- 12(1). <https://doi.org/10.1038/s41419-020-03308-w>
19. Gupta, D.; Roy, P.; Sharma, R.; Kasana, R.; Rathore, P.; Gupta, T.K. *Clin. Exp. Med.*, **2024**; *24*(1). <https://doi.org/10.1007/s10238-023-01262-3>
20. Pillay, V.; Frank, D.; Tyagi, C.; Tomar, L.K.; Choonara, Y.E.; Du Toit, L.C.; et al. *Int. J. Nanomed.*, **2014**; *9*: 589–607. <https://doi.org/10.2147/ijn.s50941>
21. Jain, V.; Kumar, H.; Anod, H.V.; Chand, P.; Gupta, N.V.; Dey, S.; et al. *J. Control. Release*, **2020**; *326*: 628–647. <https://doi.org/10.1016/j.jconrel.2020.07.003>
22. Kumar, S.; George, M.; Joseph, L. *World J. Pharm. Sci.*, **2022**; *10*(2): 216–231. <https://doi.org/10.54037/wjps.2022.100208>
23. Li, F.; Yang, X.; Yang, Y.; Li, P.; Yang, Z.; Zhang, C. *Drug Dev. Ind. Pharm.*, **2015**; *41*(11): 1777–1784. <https://doi.org/10.3109/03639045.2015.1004183>
24. Berkowitz, S.A. *AAPS J.*, **2006**; *8*(3): E590–E605. <https://doi.org/10.1208/aapsj080368>
25. Ahmad, S.; Ashwin, B.; Rahman, B.A.; Gorad, R.U.; Tare, H. *Int. J. Health Sci.*, **2022**; *6*(S4): 11450–11465. <https://doi.org/10.53730/ijhs.v6ns4.11131>
26. Dynamic Light Scattering Particle Size Distribution Analysis. HORIBA Scientific (Web source).
27. The Principles of Dynamic Light Scattering. Anton Paar Wiki (Web source).
28. Pecora, R. Springer, **1985**. <https://doi.org/10.1007/978-1-4613-2389-1>
29. Koenig, J.L. *Appl. Spectrosc.*, **1975**; *29*(4): 293–308. <https://doi.org/10.1366/000370275774455888>
30. Workman, J. *Spectroscopy*, **2024**; *22*–28. <https://doi.org/10.56530/spectroscopy.ak9689m8>
31. Kumar, A.; Khandelwal, M.; Gupta, S.K.; Kumar, V.; Rani, R. *In: Elsevier*, **2019**; 77–96. <https://doi.org/10.1016/b978-0-12-816548-5.00006-x>
32. Joseph, B.; Darro, F.; Béhard, A.; Lesur, B.; Collignon, F.; Decaestecker, C.; et al. *J. Med. Chem.*, **2002**; *45*(12): 2543–2555. <https://doi.org/10.1021/jm010978m>
33. Davoren, M.; Herzog, E.; Casey, A.; Cottineau, B.; Chambers, G.; Byrne, H.J.; et al. *Toxicol. In Vitro*, **2007**; *21*(3): 438–448. <https://doi.org/10.1016/j.tiv.2006.10.007>
34. Singh, B.; Saxena, A.K.; Chandan, B.K.; Agarwal, S.G.; Bhatia, M.S.; Anand, K.K. *Phytother. Res.*, **1993**; *7*(2): 154–158. <https://doi.org/10.1002/ptr.2650070212>
35. Singh, T.; Sinha, N.; Singh, A. *Indian J. Pharmacol.*, **2013**; *45*(1): 61. <https://doi.org/10.4103/0253-7613.106437>
36. Zhang, Y.; Li, J.; Wu, Z.; Liu, E.; Shi, P.; Han, L.; et al. *Evid. Based Complement. Alternat. Med.*, **2014**. <https://doi.org/10.1155/2014/691574>
37. Udayashankar, A.C.; Rajini, S.B.; Nandhini, M.; Suhas, Y.S.; Niranjana, S.R.; Lund, O.S.; et al. *Int. Res. J. Pharm.*, **2016**; *7*(6): 103–109. <https://doi.org/10.7897/2230-8407.07674>
38. Samudram, P.; Hari, R.; Vasuki, R.; Geetha, A.; Moorthi, P.S. *Afr. J. Biochem. Res.*, **2008**; *2*(2): 61–65.
39. Mandal, U.; Jyotirmayee, B.; Mahalik, G. *Plant Sci. Today*, **2022**. <https://doi.org/10.14719/pst.1491>
40. Zhang, H.; Zhou, X.; Sheng, N.; Cui, R.; Cui, Q.; Guo, H.; et al. *Environ. Sci. Technol.*, **2018**; *52*(21): 12809–12818. <https://doi.org/10.1021/acs.est.8b04368>
41. Farkas, N.; Kramar, J.A. *J. Nanopart. Res.*, **2021**; *23*(5). <https://doi.org/10.1007/s11051-021-05220-6>
42. Wikipedia Contributors. Zeta Potential. Wikipedia (Web source).
43. Wang, S.; Su, R.; Nie, S.; Sun, M.; Zhang, J.; Wu, D.; et al. *J. Nutr. Biochem.*, **2014**; *25*(4): 363–376. <https://doi.org/10.1016/j.jnutbio.2013.10.002>
44. Feng, Y.; Kilker, S.R.; Lee, Y. *In: Elsevier*, **2020**; 213–241. <https://doi.org/10.1016/b978-0-12-815667-4.00007-9>
45. Mahrouqi, D.A.; Vinogradov, J.; Jackson, M.D. *Adv. Colloid Interface Sci.*, **2017**; *240*: 60–76. <https://doi.org/10.1016/j.cis.2016.12.006>
46. Honary, S.; Zahir, F. *Trop. J. Pharm. Res.*, **2013**; *12*(2). <https://doi.org/10.4314/tjpr.v12i2.20>
47. Moreno, J.A.S.; Mendes, A.C.; Stephansen, K.; Engwer, C.; Goycoolea, F.M.; Boisen, A.; et al. *Carbohydr. Polym.*, **2018**; *190*: 240–247. <https://doi.org/10.1016/j.carbpol.2018.02.062>
48. Wi cek, A.E. *Colloids Surf. A*, **2007**; *293*(1–3): 20–27. <https://doi.org/10.1016/j.colsurfa.2006.07.003>
49. Marsalek, R. *APCBEE Procedia*, **2014**;

- 9: 13–17. <https://doi.org/10.1016/j.apcbee.2014.01.003>
50. Marrassini, C.; Idrissi, A.; De Waele, I.; Smail, K.; Tchouar, N.; Moreau, M.; et al. *J. Mol. Liq.*, **2015**; 205: 2–8. <https://doi.org/10.1016/j.molliq.2014.08.014>
51. Song, Y.; Cong, Y.; Wang, B.; Zhang, N. *Expert Opin. Drug Deliv.*, **2020**; 17(4): 551–571. <https://doi.org/10.1080/17425247.2020.1737671>
52. Singh, D. *Glob. J. Pharm. Pharm. Sci.*, **2018**; 6(1). <https://doi.org/10.19080/gjpps.2018.06.555679>
53. Shakeri, A.; Sahebkar, A. *Recent Pat. Drug Deliv. Formul.*, **2016**; 10(1): 7–10. <https://doi.org/10.2174/1872211309666150813152305>